

# Measuring volatile emissions from moss gametophytes: A review of methodologies and new applications

Danlyn L. Brennan<sup>1</sup>  | Leslie M. Kollar<sup>2</sup>  | Scott Kiel<sup>3</sup> | Timea Deakova<sup>3</sup> |  
 Aurélie Laguerre<sup>1</sup>  | Stuart F. McDaniel<sup>4</sup>  | Sarah M. Eppley<sup>3</sup>  |  
 Elliott T. Gall<sup>1</sup>  | Todd N. Rosenstiel<sup>3</sup> 

<sup>1</sup>Maseeh College of Engineering and Computer Science, Portland State University, Portland, Oregon, USA

<sup>2</sup>Department of Plant Biology, Michigan State University, East Lansing, Michigan, USA

<sup>3</sup>Center for Life in Extreme Environments, Portland State University, Portland, Oregon, USA

<sup>4</sup>Biology Department, University of Florida, Gainesville, Florida, USA

## Correspondence

Leslie M. Kollar, Department of Plant Biology, Michigan State University, 612 Wilson Road, East Lansing, Michigan 48824, USA.  
 Email: lesliemkollar@gmail.com

This article is part of the special issue “Methodologies in Gametophyte Biology.”

## Abstract

Mosses inhabit nearly all terrestrial ecosystems and engage in important interactions with nitrogen-fixing microbes, sperm-dispersing arthropods, and other plants. It is hypothesized that these interactions could be mediated by biogenic volatile organic compounds (BVOCs). Moss BVOCs may play fundamental roles in influencing local ecologies, such as biosphere–atmosphere–hydrosphere communications, physiological and evolutionary dynamics, plant–microbe interactions, and gametophyte stress physiology. Further progress in quantifying the composition, magnitude, and variability of moss BVOC emissions, and their response to environmental drivers and metabolic requirements, is limited by methodological and analytical challenges. We review several sampling techniques with various analytical approaches and describe best practices in generating moss gametophyte BVOC measures. We emphasize the importance of characterizing the composition and magnitude of moss BVOC emissions across a variety of species to better inform and stimulate important cross-disciplinary studies. We conclude by highlighting how current methods could be employed, as well as best practices for choosing methodologies.

## KEYWORDS

biogenic volatile organic compounds, bryophytes, gametophytes, GC-RGD, GC-ToF-MS, PTR-ToF-MS

Mosses are major components of the vegetation in many of the Earth's ecosystems, from the hottest and driest desert environments of the Mojave Desert (Tao and Zhang, 2012; Belnap et al., 2014) to the ice-free terrestrial margins of Antarctica (Prather et al., 2019). Mosses provide a habitat for numerous organisms, many of which engage in intimate ecological interactions with their moss hosts. These interactions between nonvascular plants (such as mosses) and other organisms may be mediated through the production of biogenic volatile organic compounds (BVOCs) (Farag et al., 2013; Vicheroová et al., 2020). Plant BVOCs comprise numerous compound classes, including terpenoids, benzenoids, phenylpropanoids, fatty acid-derived green leaf volatiles, nitriles, and some

organosulfides, which may contribute to secondary defense, semiochemical communication, photochemical tolerances, and other physiological responses (Bouwmeester et al., 2019). Moss BVOC emission rates are sensitive to temperature and other environmental conditions that are made less predictable by a changing climate (Rinnan et al., 2020). Ongoing efforts by the scientific community to investigate moss BVOCs are increasing our understanding of the genetic mechanisms involved (Kollar et al., 2021), informing ecology- and physiology-related questions (Monson et al., 2013; Lantz et al., 2015; Vicheroová et al., 2020; Heck et al., 2021), and identifying their important impacts on biosphere–atmosphere interactions (Faubert et al., 2010; Sharkey and Monson, 2017).

Danlyn L. Brennan and Leslie M. Kollar contributed equally to this study.

This is an open access article under the terms of the Creative Commons Attribution-NonCommercial License, which permits use, distribution and reproduction in any medium, provided the original work is properly cited and is not used for commercial purposes.

© 2022 The Authors. *Applications in Plant Sciences* published by Wiley Periodicals LLC on behalf of Botanical Society of America.

Mosses may use BVOCs to communicate within species or among a wide variety of other members of their community. In *Ceratodon purpureus* (Hedw.) Brid., fertile female gametophytes produce a wider variety and greater quantity of BVOCs than fertile male plants, with microarthropods preferentially choosing female BVOCs (Cronberg et al., 2006; Rosenstiel et al., 2012). The extent of this preference and underlying mechanisms is not well known; however, in the process of moving toward the female plants, the microarthropods likely pass through male plants and collect moss sperm. In another study, the presence of microarthropods was shown to increase the number of successfully reproducing genotypes in experimental mesocosms, and increased moss fertilization rates fivefold (Shortlidge et al., 2021). Sexually dimorphic BVOC profiles may therefore contribute to the evolution of reproductive isolation, should different species of moss attract only specific arthropods. Additionally, the sexually dimorphic selection imposed by the presence of arthropods could lead to the evolution of BVOC profiles that might contribute to the maintenance of genetic variation for fitness (Kollar et al., 2021), assuming that the optimal BVOC production differs between males and females.

Plant BVOCs also play a large role in biosphere-atmosphere interactions, including the formation and quenching cycles of tropospheric ozone, as well as the formation of secondary organic aerosols and particulate matter. Isoprene and monoterpenes are only two of the many non-methane BVOCs that drive global tropospheric chemistry, and are major players in global carbon cycles. Isoprene and monoterpenes act as reducing agents in photo-oxidative chemical reaction cycles with NO and NO<sub>2</sub>, jointly known as NO<sub>x</sub> (Fehsenfeld et al., 1992). High-NO<sub>x</sub> conditions, as well as elevated temperatures, are often found in densely populated urban areas (Ghirardo et al., 2016; Da Silva et al., 2018). Isoprene and monoterpenes make up the largest portion of hydrocarbon emissions and are the dominant non-methane BVOCs by mass, contributing about half of global emissions into the troposphere (Fehsenfeld et al., 1992; Simon et al., 2019). Trees and canopy-level emissions cannot account for the total atmospheric BVOC levels (Bracho-Nunez et al., 2013; Schallhart et al., 2018; Yan et al., 2021), suggesting that some of the remaining isoprene and monoterpenes may be derived from other sources, including mosses (Guenther et al., 1993; Arneth et al., 2008; Lin et al., 2019).

The physiological roles of plant isoprene emissions remain enigmatic (Sharkey and Monson, 2017). Similarly, the evolutionary origins of land plant isoprene emissions are uncertain (Harley et al., 1999). Among mosses, the presence, quantity, and composition of BVOC emissions have not been reported (Hanson et al., 1999; Monson et al., 2013). Testing the fitness consequences of producing metabolically expensive BVOCs will shed light on both the physiological roles and evolutionary origins of plant isoprene emissions. A prerequisite to achieving this goal is to develop robust methods for the quantification of BVOCs emitted by these ancient and ubiquitous land plants.

Here, we review four experimental approaches regularly used by our research groups to survey moss BVOCs. These methods involve the use of three different instruments along with several custom collection techniques. These methods have been used over a range of experimental designs, including both non-targeted and targeted approaches and high-throughput techniques, and can be deployed in both laboratory and field settings. First, to measure a known target compound from moss gametophytes, we used gas chromatography with a mercury oxide-based reduction gas detector (GC-RGD; Trace Analytical Laboratories, Muskegon, Michigan, USA). Second, we used a proton transfer reaction time-of-flight mass spectrometer (PTR-ToF-MS 1000; Ionicon Analytik, Innsbruck, Austria) with hydronium (H<sub>3</sub>O<sup>+</sup>) as the primary reagent for two collection methods: a high-throughput static headspace sampling method to determine an emissions factor and an automated method for simultaneous multi-species sampling to determine a dynamic flux. Lastly, using gas chromatography time-of-flight mass spectrometry (GC-ToF-MS), we designed a simple flow-through chamber that utilizes automated thermal desorption (ATD) cartridges packed with resins optimized for the collection of plant-derived BVOCs. This technique was used to identify a range of BVOCs in a single species of moss collected from the field and tested in a controlled laboratory environment. Our goal in this paper is to describe the methods available to study moss BVOCs and provide useful information that will inform decisions on experimental designs for the specific data outputs necessary to inform research.

## METHODS

### Gas chromatography with reduction gas detector (GC-RGD)

Using GC-RGD, we set up three different collection apparatuses to measure a known target compound. Each apparatus was specifically designed according to the research question. One apparatus was first used in a screening protocol to identify isoprene-emitting species from five families of mosses (Bryaceae, Dicranaceae, Ditrichaceae, Polytrichaceae, and Pottiaceae; Figure 1C, Appendix S1). Once identified, a second apparatus was used to estimate the amount of isoprene emissions from an individual *Polytrichum juniperinum* Hedw. gametophyte (Figure 1B). A third apparatus was needed to scale-up the measurement of isoprene emissions from an entire moss colony (six patches of *P. juniperinum*; Figure 1A).

The GC-RGD experiments were performed at a controlled temperature of 30°C. This temperature is a widely used standard for testing isoprene emissions in both vascular plants (Sharkey and Loreto, 1993; Monson et al., 1994; Geron et al., 2000; Bracho-Nunez et al., 2013; Sharkey and Monson, 2017) and nonvascular plants, such as *Polytrichum juniperinum* (Hanson et al., 1999; Janson

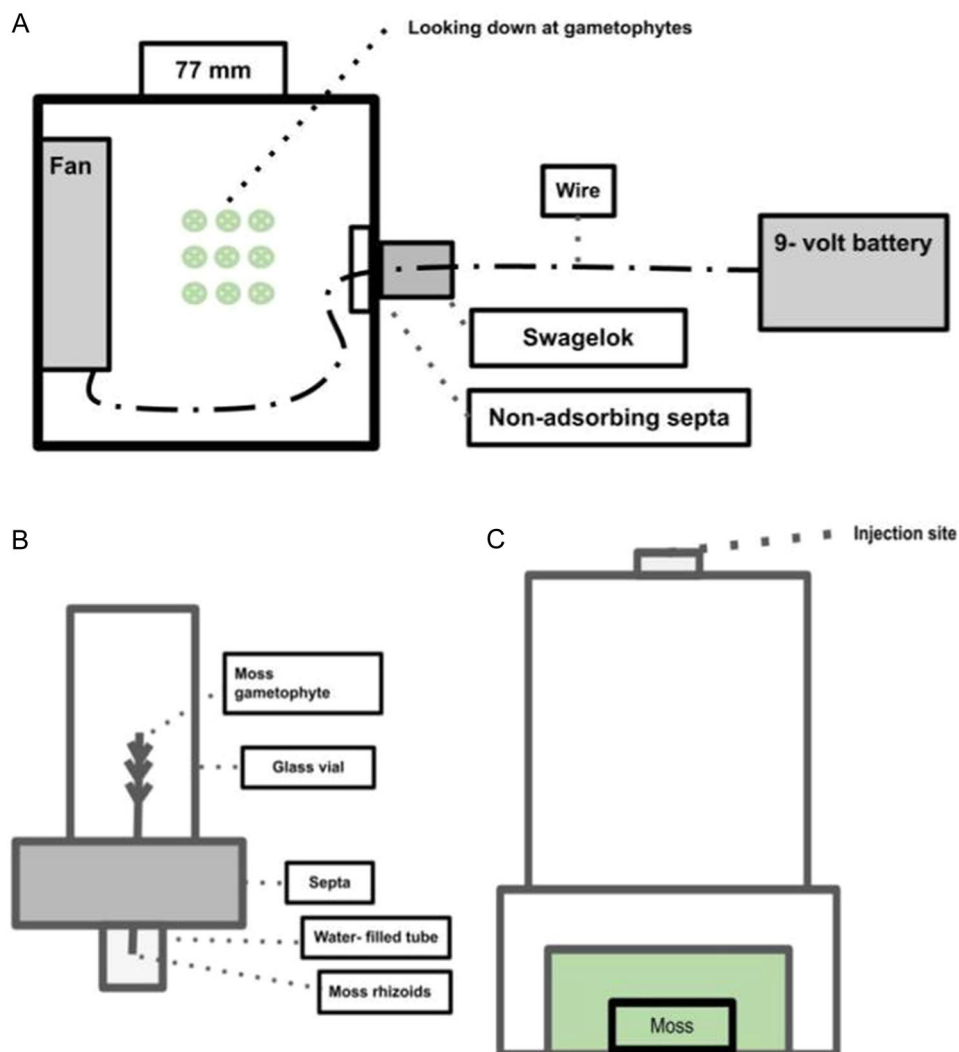


**FIGURE 1** The three collection apparatuses used in the GC-RGD. (A) Chamber for headspace analyses of the moss canopy. The wire is extended from the fan through the Swagelok and attached to the 9-V battery. This was used to ensure equal mixing of air in the chamber and avoid settling. A sampling port with septa was installed in the Swagelok. (B) The apparatus for isoprene emission assessment for individual *Polytrichum* gametophytes with rhizoids pulled through a septa and inverted in a glass vial. The rhizoid was then placed into a test tube filled with tap water to avoid dehydration. (C) Static chamber (not airtight) for isoprene emission detection. The injection site for sample extraction was through a thin indent on the top of the lid, which was immediately covered with non-adsorptive tape.

et al., 1999; Deakova, 2019). All collection methods for the GC-RGD experiments used lighting set to a standard photosynthetic photon flux density (PPFD) of  $1000 \mu\text{mol photons m}^{-2} \text{s}^{-1}$  to simulate standard conditions (Geron et al., 2000). To calibrate the GC-RGD, 1 mL of a standardized National Institute of Standards and Technology (NIST) calibration gas mixture (Linde, Dublin, Ireland; 50 ppm standard  $\text{N}_2$  with added high-purity isoprene standard) was used to create a calibration curve prior to sampling. The sampling was performed using a 2-mL Pressure-Lok Precision Analytical Syringe (VICI Precision Sampling, Baton Rouge, Louisiana, USA) to extract the gaseous headspace from the collection chambers, which was then injected into the GC inlet. Throughout this paper, we describe the emitting surface area of the entire moss colony as the moss “canopy.”

### Isoprene detection in a static accumulation chamber

For the initial isoprene screening, five families were tested, including the Polytrichaceae family, a known isoprene emitter (Hanson et al., 1999). Moss gametophyte canopy samples ( $5 \times 5 \text{ cm}$ ) were placed in sterilized PlantCon containers (MP Biomedicals, Irvine, California, USA) that were not airtight (Figure 1C). We incubated the samples for 5 min at  $30^\circ\text{C}$  before the headspace samples were taken and injected into the GC inlet.

### Isoprene flux of individual moss gametophytes

A subset of individual *Polytrichum juniperinum* moss gametophytes from each field collection (six sites in Oregon,

USA) were placed in 40-mL glass vials (Figure 1B). We accumulated emissions in the chamber headspace under these conditions for 5 min before sampling by closing the vials with a non-absorptive septa (VICI Precision Sampling). To report an emission flux, the accumulated concentrations were normalized by the accumulation time and the measured leaf surface area of the sampled gametophyte. Leaf area was measured using a Leica microscope (Leica Microsystems, Wetzlar, Germany) with an AxioCam 105 Color camera attachment (Carl Zeiss, Jena, Germany). The surface area was calculated using Zen Blue software (version 1.1.2.0; Carl Zeiss).

## Isoprene testing of intact gametophyte canopies

Canopy-level isoprene emission rates were collected from intact *Polytrichum juniperinum* moss gametophyte patches collected from six different field sites in Oregon. These canopies were collected as intact circular sheets (40 cm diameter), including a layer of soil substrate, and planted in 38-L pots filled with a sterilized propagation-grade sand and soil mix (2 : 1). The custom-built collection chamber consisted of a 77 × 77 × 97 mm polypropylene Magenta vessel (MilliporeSigma, St. Louis, Missouri, USA) fitted with Swagelok (Solon, Ohio, USA) sampling ports and sealed with non-adsorptive polytetrafluoroethylene (PTFE) septa (Figure 1A). A thermocouple for temperature observation and a 40 × 40 mm fan (9 V) were attached inside the chamber and pulsed briefly to ensure an equal mixing of the volume of the headspace, which was open to ambient air and not airtight. The static headspace was accumulated for 10 min before the extraction of the sample through the side of the vessel equipped with a septa and Swagelok sampling ports.

## Isoprene identification and quantification

Samples of 1 mL of air were removed via an analytical syringe and injected into a reduction gas detector (Trace Analytical Laboratories). The isoprene was separated isothermally (100°C) in a stainless-steel column (0.9 m × 3 mm internal diameter) packed with UNI Beads 3 S, mesh size 60/80 (Sigma-Aldrich, St. Louis, Missouri, USA).

The spectral peak identification was performed using the PEAK software (Stein, 1999), integrating the raw peak area units and retention times. Peak times and areas were recorded using a commercial integrator (Model 3396; Hewlett-Packard, Palo Alto, California, USA) and converted to parts per billion (ppb). Isoprene was identified by determining a calibration curve from an isoprene standard (MilliporeSigma). To quantify the isoprene, significant peak areas were identified following a baseline correction. We controlled for possible contamination in the background air by running concurrently collected atmospheric control blanks from empty chambers at the time of the collection

of the headspace samples. The atmospheric blank values were subtracted from the collected headspace sample to exclude any isoprene present in the local atmosphere.

We also performed quality assurance and quality control of the isoprene peak by running an isoprene Standard Reference Material (NIST SRM 1515) through the GC-RGD periodically to check for instrumental drift. The GC-RGD was calibrated for each sampling run using a calibrated analytical standard 60.8 ppm isoprene in N<sub>2</sub> gas (Praxair Surface Technologies, Indianapolis, Indiana, USA). This standard was introduced to a mixing chamber where a 10-point calibration curve was created by diluting ultra-high-purity N<sub>2</sub> at different flow rates to generate a calibration curve.

## Proton transfer reaction time-of-flight mass spectrometer (PTR-ToF-MS)

### Static headspace sampling (emission factor)

We used the PTR-ToF-MS to design a high-throughput static headspace sampling method to screen many individuals of a single moss species and generate a BVOC “fingerprint.” We collected operculate sporophyte capsules of *Ceratodon purpureus* in Portland, Oregon, and generated axenic cultures of the individual genotypes. We conducted an experiment on plants grown in a greenhouse during late summer, using a soil amendment with calcined, non-swelling illite clay (Turface MVP; Profile Products LLC, Buffalo Grove, Illinois, USA) in the bottom of each pot for wicking. For each replicate, we carefully extracted approximately 200 mg of fertile gametophytes (antheridia and archegonia) from the substrate. We placed the tissue in 5-mL vials with two drops of distilled water to avoid dehydrating the plant during the static headspace accumulation. We created several blanks (two drops of water only) for each batch of samples per collection day. We placed all prepared sample cuvettes under an LED light source at a PPFD of 1000 μmol m<sup>-2</sup> s<sup>-1</sup> for 2 h in a temperature-controlled room (20°C).

We measured the emissions at 12:00 p.m. each day using a custom cuvette system made from two airtight glass syringes designed for gas sampling (Figure 2). The inlet of one syringe connected to a mass flow controller (MC-2SLPM-D; Alicat Scientific) and the second syringe (sampling outlet) was attached to the PTR inlet via PTFE tubing. The PTR inlet was set to pull at a constant air flow rate of 50 cc min<sup>-1</sup>. A T-valve was attached between the mass flow controller and sample inlet syringe to decrease pressure by allowing excess air to move out of the system. This created a needle-plunge system where both needles would be inserted into the sample vial, with ultra-high-purity zero air (Airgas, Radnor, Pennsylvania, USA; <0.1% total hydrocarbon) flowing through the vial and the PTR sampling compounds in the vial headspace. When not measuring the emissions from a sample, the PTR-ToF-MS

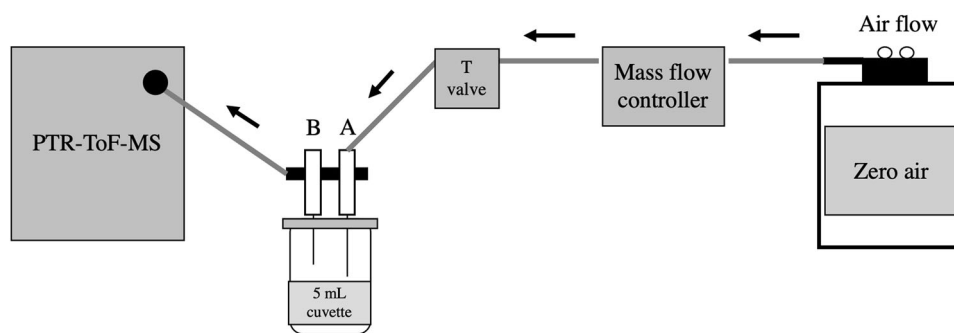


FIGURE 2 Diagram of the 5-mL sampling cuvette setup used with PTR-ToF-MS. This image was modified from Kollar et al. (2021).

inlet was supplied with a constant stream of ultra-high-purity zero air (Airgas; <0.1% total hydrocarbon) via a mass flow controller (MC-2SLPM-D; Alicat Scientific) at a rate of  $300 \text{ cc min}^{-1}$ . During the two hours of headspace accumulation, the temperature of the samples was kept at  $30^\circ\text{C}$ . Following the volatile collections, we dried the tissue for 3 d at  $35^\circ\text{C}$  in a drying oven in preparation for the dry weight measurement.

For our experiments, the drift tube conditions were 600 V,  $60^\circ\text{C}$ , and 2.09 mbar. The PTR-ToF-MS was operated at an E/N value of 138 Td. The extraction times were set for an analytical window that extended to 250 amu in 83,535 timebins. When the PTR started and the parameters were stable, we sampled the blank vial for several minutes to obtain a background noise baseline. After the blank, we tested the sample vials for 1 min each, which was equivalent to 60 1-s cycles. The instrument detected compounds in the range of 17–250 amu for compounds with a proton affinity higher than that of  $\text{H}_2\text{O}$  (e.g., many VOCs, including alkenes and oxygenated VOCs). The compounds were identified using an assigned protonated mass for each signal via a mass axis calibration, which enables the association of an ion's flight time to the compound's molecular weight. We calibrated the mass axis to three peaks:  $\text{NO}^+$  ( $m/z = 29.997$ ),  $\text{C}_3\text{H}_7\text{O}^+$  ( $m/z = 59.0497$ ), and a  $\text{C}_6\text{H}_4\text{I}_2$  fragment ( $m/z = 203.944$ ). The first two compounds are present in the instrument's drift tube due to the back-diffusion of air from the sample inlet; the instrument is sufficiently sensitive that mass axis calibration can be achieved for acetone in zero air (Airgas). The final compound ( $m/z 203.944$ ) is an internal standard continuously emitted into the drift tube from a heated permeation tube (PerMaScal; Ionicon Analytik) to provide a consistent mass axis reference calibration compound with a high molecular weight. We stored the mass spectra in 1-s intervals. We then processed the PTR data using the Ionicon Analytik PTR-MS Viewer 3.0 post-processing software.

We performed the mass assignment (identification of BVOCs) using a peak table resolved with unit mass resolution and then assigned each peak to an exact mass by inspecting the mass spectra. The resulting mixing ratio was determined using the relative transmission method described elsewhere (Holzinger et al., 2010), and used to

calculate an emissions factor normalized by dry weight ( $\text{ng s}^{-1} \text{ g DW}^{-1}$ ) for each detected mass within each sample.

### Automated flux analysis method

Additionally, we used the PTR-ToF-MS to estimate a dynamic flux across several species simultaneously. Large field-collected (Oregon) patches of moss gametophytes (*Antitrichia californica* Sull. ex Lesq., *Dicranoweisia cirrata* (Hedw.) Lindb. ex Milde, *Polytrichum juniperinum*, and *Racomitrium canescens* (Hedw.) Brid.) were planted in 100 g of perlite and peat moss substrate mix in polypropylene pots (11.4 cm in diameter, 10.2 cm deep). All moss pots were acclimated in a greenhouse for approximately one month before the experimental measurements were collected. The greenhouse was kept at ambient temperature (average temperature of  $\sim 2.9^\circ\text{C}$ ) and the mosses were watered on a twice-daily schedule. We designed an array of high-throughput dynamic headspace sampling chambers to measure the moss BVOC emission flux.

The chamber-in-chamber system consisted of an array of eight (19.1 cm tall and 14.7 cm in diameter) round acrylic glass (poly(methyl methacrylate)) test chambers. This multi-chamber system allowed for the sampling of seven pots and one empty chamber (control) per set (Figure 3). All eight test chambers were exposed to the same controlled light intensity ( $1000 \mu\text{mol m}^{-2} \text{ s}^{-1}$ ), and the test chamber inlet air temperature was held within a range of  $25\text{--}30^\circ\text{C}$ . Near-ambient  $\text{CO}_2$  levels ( $471.28 \text{ ppm} \pm 6.28 \text{ SD}$ ) and <80% relative humidity levels were maintained. The environmental chamber conditions were monitored while ambient  $\text{CO}_2$  was measured with a  $\text{CO}_2$  gas sensor (LI-840A  $\text{CO}_2/\text{H}_2\text{O}$  Gas Analyzer; LI-COR Biosciences, Lincoln, Nebraska, USA) at the chamber's outlet.

The LED lamps used to set the light conditions necessitated the integration of air conditioning into the larger chamber enclosing the test chambers to keep the temperature within the target range throughout the entirety of the experiment. To minimize any potential leaks into and out of the chambers, a piece of parafilm 17.8 cm in length was wrapped around the bottom seal. Leak tests were performed to ensure that losses were insignificant (<10% of the flow). All flow lines connecting the PTR-ToF-MS inlet to the experimental chambers consisted

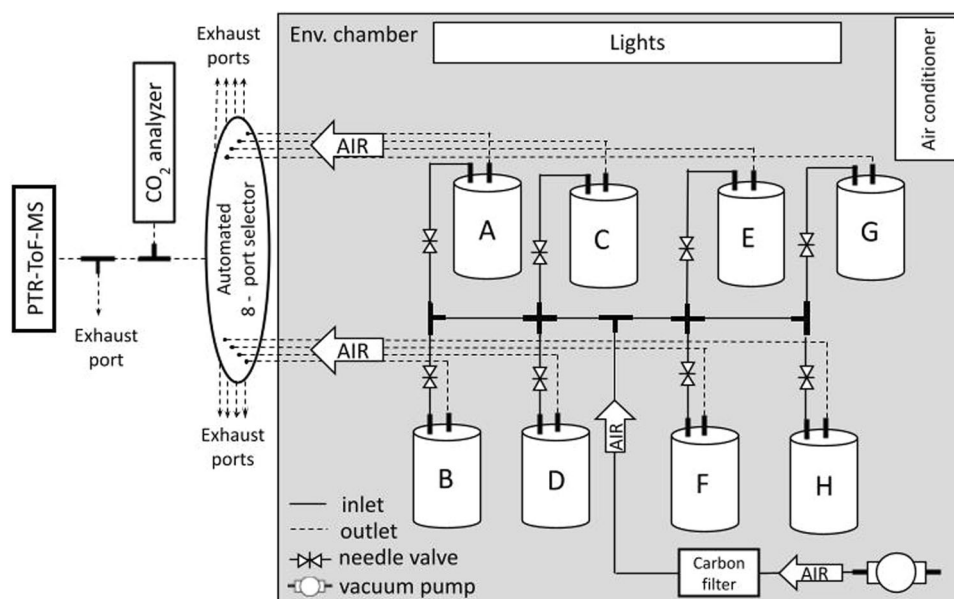


**FIGURE 3** Schematic of the environmental chamber with eight sampling chambers in a parallel flow configuration (A–H). Light and temperature conditions were controlled by the lamp and air conditioner inside the environmental chamber. All inlet air flow induced by the pump was first passed through a carbon trap filter to remove background BVOCs.

of 1/4-in (6.4-mm) outer diameter (OD) perfluoroalkoxy alkane tubing. Each of the eight chambers were equipped with flow lines attached to an inlet and outlet fitted with Swagelok bulkhead unions (1/4 in [6.4 mm]; model SS-400-61) with a Viton O-ring (013 Viton O-Ring, 75 A durometer, black, 7/16 in [1.1 cm] ID, 9/16 in [1.4 cm] OD, 1/16 in [0.2 cm] width; Viton, Wilmington, Delaware, USA) to create a seal around the bulkhead unions. Individual needle valves (Stainless Steel Integral Bonnet, 0.37 Cv, 1/4 in [6.4 mm], Swagelok tube fitting, regulating stem; Swagelok) were installed upstream of each chamber, allowing for the adjustment of individual flow rates.

Each test chamber outlet ran to an individual port in an eight-port flow-through actuator and selector (model EUTB-2VLSF8MWE2; Valco Instruments, Houston, Texas, USA) controlled to allow the PTR-MS inlet to sample from each outlet line from the test chambers. The acquisition time for each chamber was 3 min. The PTR-ToF-MS drift tube conditions were set to a multiplier voltage of 600 V, temperature of 60°C, and 2.2 mbar pressure. The PTR-ToF-MS was operated at an E/N value of 135 Td.

We loaded samples into seven of the eight inner chambers. All eight chambers were placed below the lamps as close together as possible for even lighting exposure. The chamber conditions were set and allowed to reach a steady state before commencing the experiment. The flow rates in each chamber were adjusted and recorded for later calculations. The target flow rate for each chamber was 1200 standard cubic centimeters per minute (SCCM).

Each of the moss and substrate samples was measured at the same time of day (12:00 p.m.) for four consecutive days. We measured each set for 30 min. Each chamber was

sampled for 3 min, collecting data at one cycle per second. The total concentration of monoterpenes was determined by summing the masses for  $(C_{10}H_{16})H^+$  ( $137.1325 \text{ g mol}^{-1}$ ) with the fragment  $(C_6H_8)H^+$  ( $81.07043 \text{ g mol}^{-1}$ ), as suggested by Materić et al. (2015).

### Gas chromatography time-of-flight mass spectrometry (GC-ToF-MS)

#### Dynamic headspace sampling with automated thermal desorption (ATD)

In order to collect BVOCs from mosses in their natural habitats, we used the GC-ToF-MS method with ATD cartridges (Camsco, Houston, Texas, USA) to sample a range of BVOCs in a single species of moss. Chambers were designed and fabricated for BVOC collection to allow for the collection of samples onto the ATD cartridges (Figure 4). Two 3/8-in (1.0-cm) Swagelok bulkhead fittings were sonicated in a 50/50 (v/v) hexane/acetone solution and dried at 150°C for 90 min before being installed onto the containers. Teflon washers were used to create a seal around the bulkheads, and 1/4-in (6.4-mm) Teflon tubes were cut to adjust the height of flow inlet and outlet within the chamber. The ATD cartridges were attached to the bulkheads to simultaneously collect background air at the inlet and BVOCs from within the chamber at the outlet.

Before the BVOC collection, the stainless steel ATD cartridges were conditioned by reverse-flow ultra-high-pressure N<sub>2</sub> at 150°C for 30 min and 300°C for 1 h. Each conditioned cartridge was sealed with a 3/8-in (1.0-cm) end cap (Swagelok) fitted with Teflon ferrules cleaned with

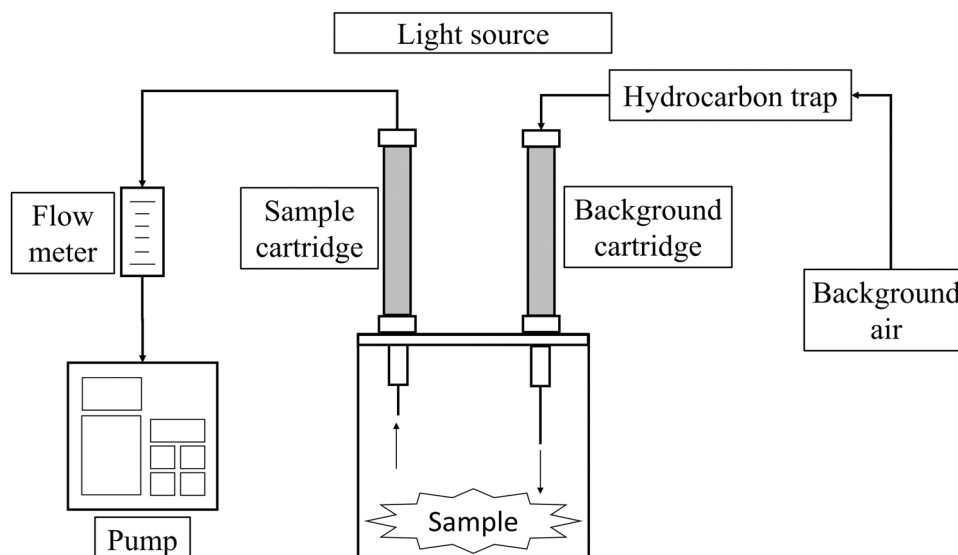


FIGURE 4 Diagram of the sampling chamber used with the ATD cartridges for collection in the field or laboratory.

methanol and water. All of the ATD cartridges used for this experiment were packed with two layers of adsorbing resin consisting of 100 mg Tenax (Viganò, Italy) TA 35/60 and 120 mg Carbograph 1TD 60/80. These resins were previously shown to have a good retention of a wide range of plant-derived BVOCs (Pankow et al., 2012).

Six species of moss were selected to be tested for a range of BVOC compounds: *Polytrichastrum alpinum* (Hedw.) G. L. Sm., *Sanionia georgicouncinata* (Müll. Hal.) Ochyra & Hedenäs, *Ceratodon purpureus*, *Bryum pseudotriquetrum* (Hedw.) G. Gaertn., B. Mey. & Scherb., *Syntrichia magellanica* (Mont.) R. H. Zander, and *Chorisodontium aciphyllum* (Hook. f. & Wilson) Broth. Moss patches were excised directly from larger patches in the field and cut to 35 cm<sup>2</sup> to fill the sampling chamber. Conditioned ATD cartridges were attached to the inlet and outlet of the sampling chamber. A hydrocarbon trap was added to the inlet cartridge to clean the airstream before it entered the chamber. An LED light source was set to a PPF of 1000 μmol m<sup>-2</sup> s<sup>-1</sup> and placed over the clear chamber containing the moss tissue for the duration of the experiment. The chamber outlet was attached to a portable pump with low-power consumption (model 224-PCXR8; SKC, Blandford Forum, United Kingdom) and set to a flow of 100 mL min<sup>-1</sup> for 60 min. Once the sampling was complete, the cartridges were sealed with end caps and placed in a precleaned Teflon container until subjected to the analysis.

### Comprehensive moss BVOC profile using GC-ToF-MS

Compounds were desorbed using a TurboMatrix 650 ATD (PerkinElmer, Waltham, Massachusetts, USA) thermal desorption apparatus and analyzed with GC-ToF-MS to generate a comprehensive BVOC profile. Each ATD cartridge was injected with a previously prepared internal standard gas

mixture containing fluorobenzene, toluene-d<sub>8</sub>, bromofluorobenzene, and 1,2-DCB-d<sub>4</sub> (1,2-dichlorobenzene-d<sub>4</sub>) in ultra-high-pressure N<sub>2</sub>. A fused silica transfer line was used to connect the TurboMatrix to the GC injector and heated to 225°C. The ATD cartridges were heated to 275°C to thermally desorb the BVOCs of the resins onto a focusing trap for 10 min at a flow rate of 30 mL min<sup>-1</sup>, which was then desorbed at 295°C for 3 min before being injected into the GC column.

A 60-m DB-VRX capillary column (Agilent Technologies, Santa Clara, California, USA) with an ID of 250 μm was previously found to be effective in separating a large number of biogenic compounds with good resolution (Pankow et al., 2012). The carrier gas flow through the column was set to 1 mL min<sup>-1</sup>. The GC oven temperature was initially set at 45°C for the first 5 min, then raised by 10°C min<sup>-1</sup> until 190°C was reached, after which the rate was reduced to 5°C min<sup>-1</sup> until the maximum temperature of 250°C was achieved, for a total duration of about 40 min per sample. A secondary oven was used with the same temperature increase but offset by 20°C. The detector voltage was set to 1500 V and the ion source temperature was set to 225°C.

The initial identification of compounds was achieved by detecting NIST library matches provided from databases included with the GC software. Each detected compound was manually checked for the accuracy of the fragmentation patterns from multiple library hits. It is recommended that three replicates are collected for each treatment and species of moss to maximize the accuracy of the fragmentation patterns and library hits between samples.

## RESULTS

All of the instrumental methods and different sampling techniques used resulted in the identification of BVOCs. The GC-RGD approach was able to detect differences in

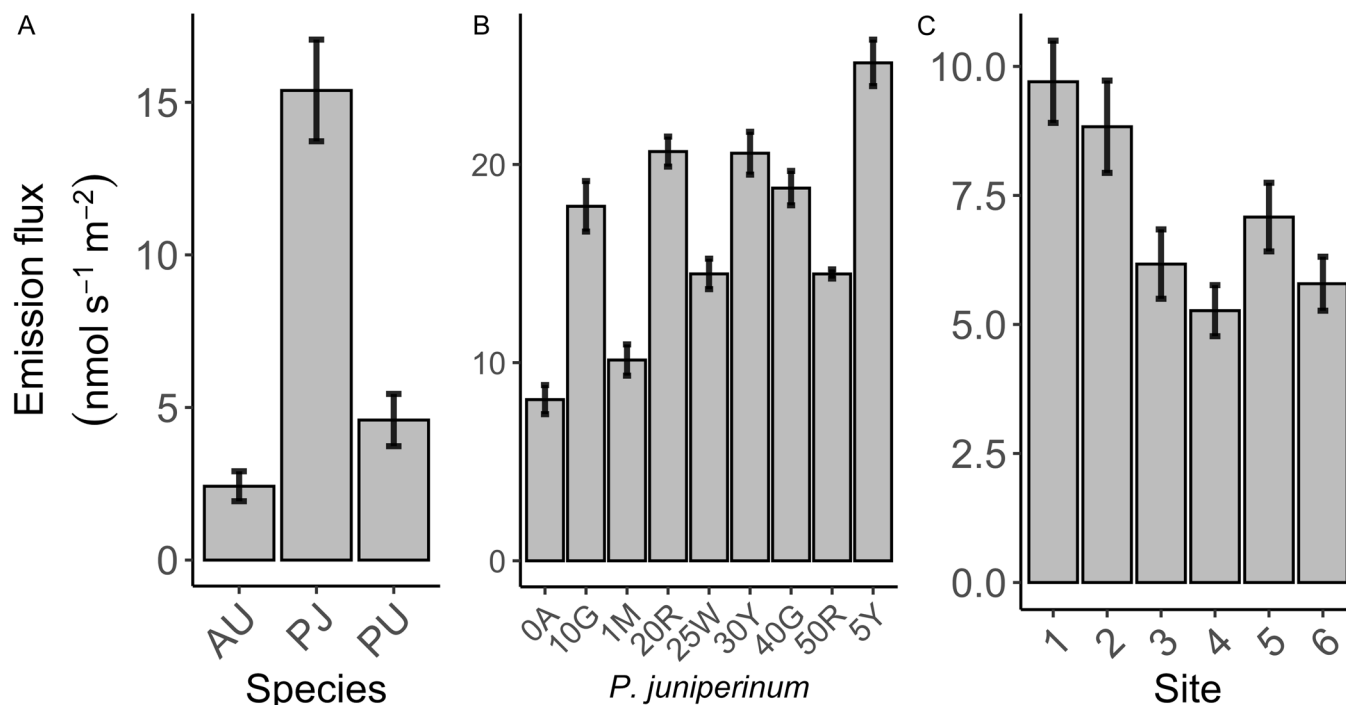


**FIGURE 5** Isoprene emissions from selected species. (A) Screening isoprene emissions in *Atrichum undulatum* (AU,  $n = 70$ ), *Pogonatum urnigerum* (PU,  $n = 41$ ), and *Polytrichum juniperinum* (PJ,  $n = 55$ ) gametophytes. (B) Isoprene emission across eight samples of individual *P. juniperinum* gametophytes ( $n = 45$ ). (C) Canopy-level isoprene emissions of *P. juniperinum* at six different locations (across all locations  $n = 166$ ). All error bars represent standard error.

isoprene emissions among species representing five families of mosses, with the highest emissions detected in the Polytrichaceae family. *Polytrichum juniperinum* had mean isoprene emissions of  $15.39 \text{ nmol m}^{-2} \text{ s}^{-1} \pm 1.42 \text{ SE}$  ( $n = 55$ ; Figure 5A, Appendix S2). At the canopy level, the emissions of this species varied across the six field sites: (1)  $9.70 \text{ nmol m}^{-2} \text{ s}^{-1} \pm 0.8 \text{ SE}$  ( $n = 48$ ), (2)  $8.83 \text{ nmol m}^{-2} \text{ s}^{-1} \pm 0.90 \text{ SE}$  ( $n = 31$ ), (3)  $6.17 \text{ nmol m}^{-2} \text{ s}^{-1} \pm 0.68 \text{ SE}$  ( $n = 39$ ), (4)  $5.27 \text{ nmol m}^{-2} \text{ s}^{-1} \pm 0.50 \text{ SE}$  ( $n = 43$ ), (5)  $7.08 \text{ nmol m}^{-2} \text{ s}^{-1} \pm 0.67 \text{ SE}$  ( $n = 39$ ), (6)  $5.79 \text{ nmol m}^{-2} \text{ s}^{-1} \pm 0.53 \text{ SE}$  ( $n = 39$ ; Figure 5C, Appendix S3). For the individual *P. juniperinum* gametophytes, mean isoprene emissions levels of  $16.92 \text{ nmol m}^{-2} \text{ s}^{-1} \pm 1.42 \text{ SE}$  ( $n = 45$ ; Figure 5B, Appendix S4) were detected.

The emissions factors of the BVOCs in *Ceratodon purpureus* were estimated by PTR-ToF-MS in units of total concentration over the time of accumulation, using methods described by Kollar et al. (2021). These data resulted in the identification of 75 different volatile compounds by their mass-to-charge ratio ( $m/z$ ). The resolution of individual BVOCs as masses is limited because some likely contain many isomers. The total masses detected over the sampling time showed that males emit fewer compounds than females under the sampling conditions (Figure 6). In a different experiment using PTR-ToF-MS to measure emission fluxes, we observed differences in the BVOCs between species, with an elevated isoprene emission flux from *Polytrichum*

*juniperinum* (POL) (isoprene  $656.79 \mu\text{g h}^{-1} \text{ m}^{-2} \pm 167.50 \text{ SE}$  and monoterpenes  $2.53 \mu\text{g h}^{-1} \text{ m}^{-2} \pm 0.46 \text{ SE}$ ,  $n = 4$ ; Figure 7, Appendix S5) and relatively lower emissions fluxes from the other species, particularly *Racomitrium canescens* (isoprene  $7.86 \mu\text{g h}^{-1} \text{ m}^{-2}$ ,  $2.18 \text{ SE}$  and monoterpenes  $1.60 \mu\text{g h}^{-1} \text{ m}^{-2}$ ,  $0.3 \text{ SE}$ ,  $n = 4$ ; Figure 7, Appendix S5).

Of the six moss species analyzed using GC-ToF-MS with ATD cartridge sampling, *Chorisodontium aciphyllum* was selected as an illustrative example of the data acquired. The analysis of *C. aciphyllum* resulted in the identification of 103 BVOCs, which were binned into compound classes based on functional groups (Figure 8, Appendix S6). The largest contribution came from alkanes ( $41.43\% \pm 2.76 \text{ SE}$ ,  $n = 3$ ), arenes ( $20.16 \pm 1.62 \text{ SE}$ ,  $n = 3$ ), and alkenes ( $14.41\% \pm 0.35 \text{ SE}$ ,  $n = 3$ ). The terpenoid compounds mainly consisted of isoprene and monoterpenes ( $5.53\% \pm 0.69 \text{ SE}$ ,  $n = 3$ ). The five least abundant compound classes were nitriles ( $1.96\% \pm 0.14 \text{ SE}$ ,  $n = 3$ ), ethers ( $1.35\% \pm 0.21$ ,  $n = 3$ ), organosulfur ( $1.14\% \pm 0.31 \text{ SE}$ ,  $n = 3$ ), organic acids ( $0.61\% \pm 0.03\% \text{ SE}$ ,  $n = 3$ ), and esters ( $0.33\% \pm 0.32 \text{ SE}$ ,  $n = 3$ ).

## DISCUSSION

Mosses are a major component of Earth's major ecosystems, providing a critical habitat for many organisms. Moss BVOC emissions could play an important role in



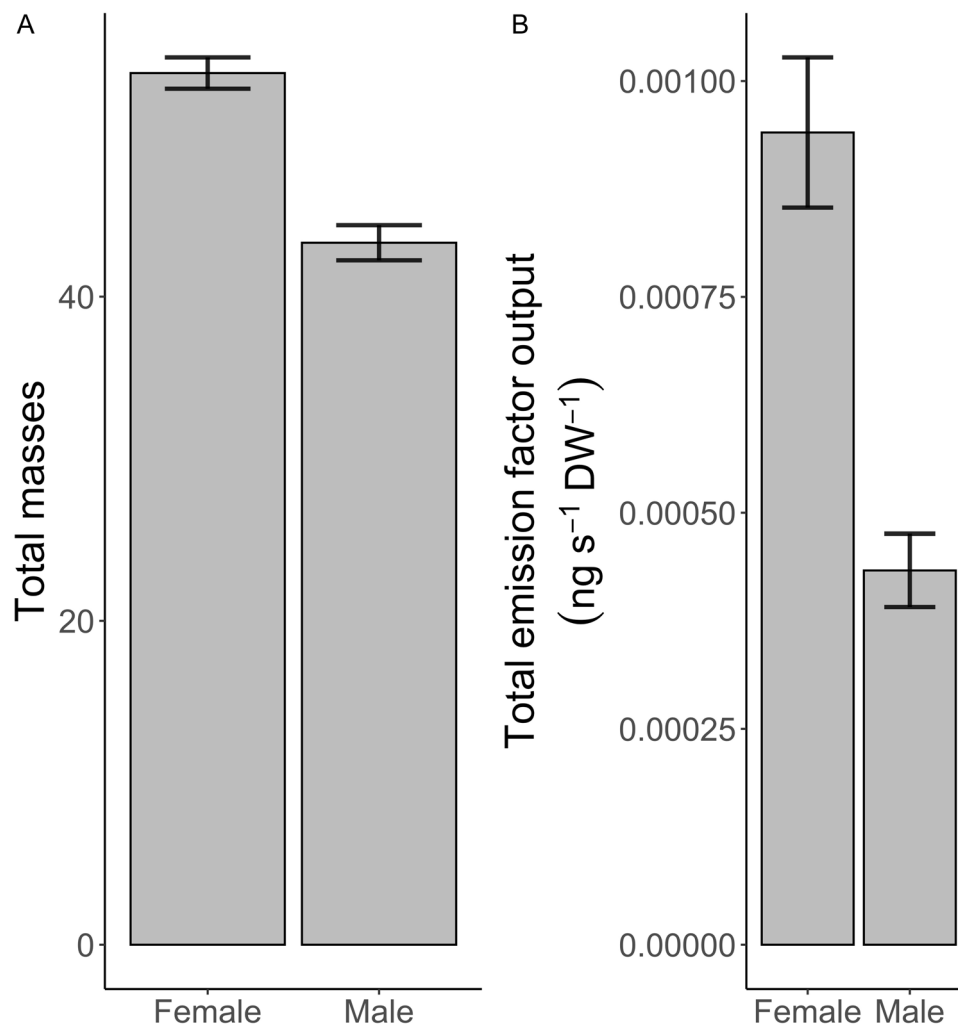


**FIGURE 6** Boxplots of the 75 masses identified in *Ceratodon purpureus* using emission factors generated from the PTR-ToF-MS. (A) Total number of masses in male ( $n = 179$ ) and female ( $n = 173$ ) gametophytes. (B) Total emission factor output across all masses in males ( $n = 179$ ) and females ( $n = 173$ ). All error bars represent standard error.

orchestrating interspecies interactions and atmospheric chemistry, among other phenomena; however, moss BVOC emissions remain understudied with respect to both the diversity of their compounds and their potential contribution to global emissions. Although these compounds have been analyzed in vascular plant emissions, such methods have rarely been applied to moss BVOC collections. The techniques and sampling strategies required to meet the specific challenges posed when characterizing moss BVOCs cannot be “off the shelf” solutions, and must be modified to address the system's unique characteristics. Here, we aim to inform scientists of the potential challenges and nuances of measuring BVOC emissions in moss gametophytes. We focus on three major questions when designing a moss BVOC experiment: (1) Can the measurement be performed in the lab or will a field-based approach be needed? (2) What type of sampling chamber is best for the application? (3) Which instrument gives what type of data, and what can that data be used for?

A major limitation in studying plant BVOCs is the difficulty of carrying out experiments under natural environmental conditions (i.e., field assays). The PTR-ToF-MS approach is often employed in the field for air-quality experiments due to its high-frequency analysis and non-target profiling capabilities, although the cost and logistics of transporting and maintaining the instrument present additional challenges. While all the described methods can be used in the field, the ATD sampling cartridge in combination with GC-ToF-MS is the most flexible solution. Remote sampling techniques with ATD cartridges can be utilized in static or dynamic flow chambers and with NIST or other structural libraries, as the mass spectral analysis provides accurate mass identification. An analysis using ATD cartridges requires standards of a target compound or a mix of similar compounds for quantification; however, when standard compounds are not available, relative abundance is often used to compare the relative emission flux of compounds. These data are often useful even when quantification is

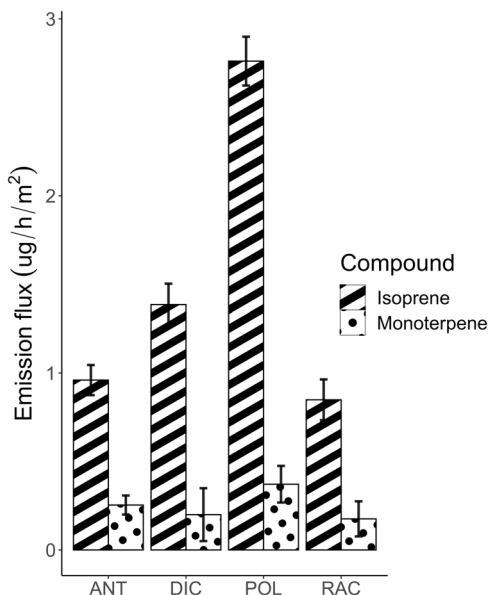


**FIGURE 7** Fluxes of four species of moss, *Antitrichia californica* (ANT,  $n = 4$ ), *Dicranoweisia cirrata* (DIC,  $n = 4$ ), *Polytrichum juniperinum* (POL,  $n = 4$ ), and *Racomitrium canescens* (RAC,  $n = 4$ ). Comparisons of isoprene and monoterpene emissions show a high overall emission from *P. juniperinum*. All error bars represent standard error.

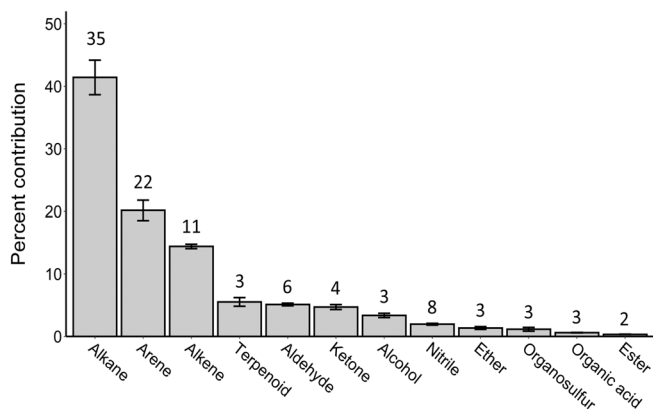


**FIGURE 8** Percentage contribution of BVOC functional groups for *Chorisodontium aciphyllum*. Percentage contribution is calculated from the relative abundances from raw spectra data with standard error ( $n = 3$ ). Individual compounds were binned into compound classes and the number of compounds per class is shown by the number above each bar.

estimated, thus providing an overall “fingerprint” of BVOC emissions from the mosses.

Another lightweight alternative to ATD cartridges is solid-phase microextraction (SPME) fiber, which can be exposed to the headspace sample and later analyzed using GC-MS. This method was used for mosses in a study by Rosenstiel et al. (2012), and was shown to provide peak separation and accurate compound identification. An advantage of SPME is that the extraction is rapid, can usually be performed without solvents, and the detection limits can reach parts per trillion (ppt) levels for certain compounds. Both the ATD cartridge and SPME

fiber allow for field-site experiments, which can be performed without the need to have a GC-MS instrument on location. When properly stored, the samples can be analyzed later in the laboratory without significant loss of volatiles (Spietelun et al., 2013). The ATD cartridges are a convenient tool for sample storage because they are composed of resins that prevent intermolecular reactions.

The ATD cartridges and SPME fibers are reusable and beneficial for BVOC storage, but they need to be properly cleaned and stored to minimize degradation. The variability in the extraction material exposed to past collections can lead to a significant amount of background signal on the cartridge and may not represent the BVOCs present in the experiment. As ATD cartridges age, the absorption and desorption process degrades the collection material. The SPME fibers also tend to be brittle. Although the chamber design is typically specific to the amount of tissue and location of sampling, it is important to use a low-VOC-emitting material, such as borosilicate glass, PTFE, or Viton, to ensure the level of background VOCs is low. This limits the potential reactions between the BVOCs and the material and allows the adoption of an appropriate sampling strategy involving blanks and empty chamber controls.

Appropriate headspace accumulation is important to ensure the concentration of sample BVOCs exceeds that of the background for the accurate estimation of emissions. The relatively small overall biomass of moss gametophytes can present a challenge to generating a concentration of BVOC emissions sufficient for a clear signal above background concentrations. To overcome this, the ratio of moss tissue to the volume of the sampling vessel should be high enough to ensure the concentration of BVOCs is detectable above the background signal. Chamber design plays a critical role in data interpretation as it is dependent on the static or dynamic nature of the headspace sampling technique. Static headspace sampling is ideal for high-throughput screening of large numbers of samples (Kollar et al., 2021). Although useful in high-throughput screening, headspace BVOC accumulation also has limitations. Over time, the accumulation of BVOCs in a small static vial or chamber may reach equilibrium with tissue emissions, potentially leading to an underestimation of the overall emission rates. To negate this problem, researchers can identify a sampling incubation period that would enable BVOC emissions to be detected before headspace equilibrium occurs.

In contrast, dynamic flow-through chamber designs allow for the quantification of real-time BVOC emissions without pressure limitations when the headspace equilibrium is reached in a fixed volume and without the subsequent feedback inherent in static headspace sampling. The PTR-ToF-MS is unique because it can measure the concentration in “real time,” allowing the calculation of dynamic BVOC emission rates or fluxes (flow of mass abundance emissions per unit time) from a chamber test. The GC-RGD and GC-ToF-MS can still provide an estimate of the emission rate using a static accumulation of BVOCs

over a given time interval. As the diffusion of BVOCs from moss tissue occurs over a concentration gradient, their accumulation eventually reaches equilibrium within a static chamber; the concentration at that point might still be a conservative estimate of a true flux. Over time, in a small static environment, the concentration gradient between the interior of the moss and the headspace will be reduced in comparison with a real open-flow scenario, in which the moss is emitting into the atmosphere. This would result in a conservative estimate of BVOC fluxes from static chambers compared with dynamic chambers. In this way, dynamic fluxes could be used to explore how emission rates change over a short time or in response to a shift in environmental conditions (e.g., light and temperature).

For all analytical methods described, it is also important to note that emission rates can be normalized by values other than leaf area. Although leaf area measurements help to accurately quantify the BVOC emissions from the surface of the tissue, emission factors (which normalize rates over other quantifiable measurements such as dry weight) also have many useful applications. It should be noted that the emissions of volatiles are likely to be different between fertile and infertile individuals of the same species and, as a result, emissions may be localized to the zones where sexual organs are situated. This would mean the traditional quantifiable measures of leaf area or dry weight may have little relevance, depending on the nature of the study, and is an area of ongoing investigation.

Instrument choice plays a major role in allowing for the collection to occur in a short time period, keeping the sampling within a consistent diurnal time schedule. In our dynamic flux PTR-ToF-MS experiment, the collection design incorporated an array of eight flow chambers to sample larger patches of gametophyte tissue, which provided a sufficient ratio of biomass to chamber volume for concentrations greater than the signal to background concentrations. Eight moss species were able to be sampled simultaneously with an automated selector to switch between each chamber. This allowed for a relatively fast collection within a 30-min window, enabling the sampling and comparison of multiple species during entire circadian cycles. Experiments that take place over 24 h or longer should consider practical issues like condensation in sampling lines. When 24-h sampling tests were performed, condensation accumulated in the Teflon tubing connected to the inlet. Depending on the length and temperature of the delivery line to the inlet, an increase in sampling time may also increase the risk of the delivery of water into the intake, which would result in a disruption in the signal and potential damage to the instrument. The PTR-ToF-MS is comparable to the GC-RGD in this regard because both have a high detection sensitivity and are time-efficient for large sample sets. As described in the PTR-ToF-MS method, a high-throughput emission factor protocol was performed in a study by Kollar et al. (2021), where they replicated finding sex-specific BVOCs in a comparison with the 2D GC-ToF-MS method described by Rosenstiel et al. (2012).

The GC-RGD also allowed for the quick screening of isoprene emission from many moss species in a relatively short time compared with the long analysis time of the GC-ToF-MS method.

The trade-offs in dynamic vs. static sampling as well as quantification vs. identification analyses are specific to the research question and should guide the choice of method. The advantages of collecting real-time fluxes with PTR-ToF-MS include the increased time resolution, which provides deeper insights into BVOC emission rates under dynamic conditions. Collectively, PTR-ToF-MS can be incorporated across many study systems (low and high emitters) and output different types of data (i.e., emission factor and real-time flux). The low emission rates in *Ceratodon purpureus* were compensated through a static headspace design as opposed to dynamic headspace, thus forfeiting the real-time flux PTR-ToF-MS method. To reach detection thresholds, a collection cuvette small enough to saturate the headspace with a limited amount of tissue was needed. With a limited amount of tissue, the instrument's rapid analysis and sensitivity (200 cps/ppbv for  $m/z$  181) enabled collection across a relatively large number of samples that emit a small quantity of BVOCs in comparison with other plant systems.

Proton reaction theory provides a fairly accurate mass identification that does not require a calibration curve for each experiment if the ToF conditions remain constant (Romano and Hanna, 2018). In cases where accurate identification is not a priority, the execution of the experiment is less time consuming because it is possible to conduct a quantitative analysis without using the specific calibration standards needed for quantification using the GC-RGD and GC-ToF-MS methods; GC-RGD and GC-ToF-MS lack the capability of real-time and direct quantitative analysis. Choosing a combined approach, such as PTR-ToF-MS and GC-ToF-MS, is useful for compound identification or quantification. Using these complementary analytical techniques allows for the real-time identification and quantification of a broad range of masses.

The mass resolving power of the PTR-ToF-MS 1000 enables greater than a  $1500 \text{ m } \Delta m^{-1}$  (FWHM) (for  $m/z > 79$ ) unit mass resolution, providing a high resolving power for comprehensive mass identification. Note that the sensitivity and mass resolving power of ToF-MS instruments can be substantially greater than those presented in this work, and may enable different sampling configurations (e.g., requiring less sample mass to achieve detectable signals) and greater insight into the chemical composition of emissions. Although a comprehensive list of masses can be identified with PTR-ToF-MS, the data still do not provide the compound identification confirmation achieved by the GC-ToF-MS. The limitations of the PTR-ToF-MS methods are due in part to the mechanisms of the detection of masses, which are predominantly identified based on the protonated molecular mass, assuming "soft" ionization.

The strength of the concurrent PTR-ToF-MS with GC-ToF-MS method comes from the GC column's ability to further partition these masses based on the chemical structure of the isomer along with fragmentation pattern

identification using the NIST library. In this respect, the use of GC-RGD or GC-ToF-MS is necessary during preliminary screening to confirm the correct identification of the detected chemical compounds before their quantification is possible. When conducting research using the GC-ToF-MS technique, a parallel application of PTR-ToF-MS for the quantitative analysis is recommended if knowledge of the transient BVOC concentrations is needed. Regardless of whether the PTR-ToF-MS equipment is used as a second detector in a GC-RGD or GC-ToF-MS system or as a separate device, this and prior studies (Yener et al., 2016) show it can be used to rapidly quantify selected masses. A benefit of solely using the PTR-ToF-MS is that it can eliminate the need for conducting a calibration curve for each experiment, which can save the researcher a considerable amount of time.

In summary, we have reviewed several of the currently employed approaches to investigating BVOC emissions from mosses. Although the selection of the sampling method and analytical framework is likely to be influenced by a suite of factors, choosing the best method requires a consideration of the three characteristics reviewed here. First, where will measurements be occurring and what access to instrumentation is available? Second, is static headspace or dynamic sampling required and how will the chamber and sampling conditions be optimized to detect BVOCs? Third, given the expected detection levels, how much sampling and replication is sufficient to identify a difference between sampling classes? This review seeks to provide others with the background to explore moss BVOC emissions, and in doing so generate new insights across a range of disciplines.

#### AUTHOR CONTRIBUTIONS

L.M.K., D.L.B., S.K., A.L., and T.D. designed the methodologies in collaboration with S.F.M., E.T.G., S.M.E., and T.N.R. All authors contributed to writing and editing the manuscript and approved the final version.

#### ACKNOWLEDGMENTS

The authors thank the anonymous reviewers for their thoughtful and thorough feedback. This work was supported by the National Science Foundation (NSF; grants 2010769 to L.M.K., 1701915 to L.M.K. and S.F.M., 1542609 to S.F.M., and 1341742 to S.M.E. and T.N.R.). D.L.B. was funded through the National Institutes of Health (NIH) as an EXITO scholar (RL5: 5RL5GM118963 and TL4: 5TL4GM118965).

#### DATA AVAILABILITY STATEMENT

Data for the PTR-ToF-MS emission factor experiment can be found at <https://doi.org/10.5061/dryad.59zw3r266>; all other data used in this article can be found in the supporting information.

#### ORCID

Danlyn L. Brennan  <http://orcid.org/0000-0001-5739-9735>

Leslie M. Kollar  <http://orcid.org/0000-0001-8726-9085>

Aurélien Laguerre  <http://orcid.org/0000-0002-8167-3586>  
 Stuart F. McDaniel  <http://orcid.org/0000-0002-5435-7377>  
 Sarah M. Eppley  <http://orcid.org/0000-0002-2094-9454>  
 Elliott T. Gall  <http://orcid.org/0000-0003-1351-0547>  
 Todd N. Rosenstiel  <http://orcid.org/0000-0001-9355-6574>

#### REFERENCES

- Arneth, A., R. K. Monson, G. Schurgers, Ü. Niinemets, and P. I. Palmer. 2008. Why are estimates of global terrestrial isoprene emissions so similar (and why is this not so for monoterpenes)? *Atmospheric Chemistry and Physics* 8(16): 4605–4620.
- Belnap, J., D. M. Miller, D. R. Bedford, and S. L. Phillips. 2014. Pedological and geological relationships with soil lichen and moss distribution in the Eastern Mojave Desert, CA, USA. *Journal of Arid Environments* 106(July): 45–57.
- Bouwmeester, H., R. C. Schuurink, P. M. Bleeker, and F. Schiestl. 2019. The role of volatiles in plant communication. *The Plant Journal* 100(5): 892–907.
- Bracho-Nunez, A., N. M. Knothe, S. Welter, M. Staudt, W. R. Costa, M. A. R. Liberato, M. T. F. Piedade, and J. Kesselmeier. 2013. Leaf level emissions of volatile organic compounds (VOC) from some Amazonian and Mediterranean plants. *Biogeosciences* 10(9): 5855–5873.
- Cronberg, N., R. Natheva, and K. Hedlund. 2006. Microarthropods mediate sperm transfer in mosses. *Science* 313(5791): 1255.
- Da Silva, C. M., S. M. Corrêa, and G. Arbilla. 2018. Isoprene emissions and ozone formation in urban conditions: A case study in the city of Rio de Janeiro. *Bulletin of Environmental Contamination and Toxicology* 100: 184–88.
- Deakova, T. 2019. Isoprene emission in Polytrichaceae mosses. PhD dissertation, Portland State University, Portland, Oregon, USA. Website: <https://doi.org/10.15760/etd.6860> [accessed 17 February 2022].
- Farag, M. A., H. Zhang, and C.-M. Ryu. 2013. Dynamic chemical communication between plants and bacteria through airborne signals: Induced resistance by bacterial volatiles. *Journal of Chemical Ecology* 39(7): 1007–1018.
- Faubert, P., P. Tiiva, Å. Rinnan, J. Räsänen, J. K. Holopainen, T. Holopainen, E. Kyrö, and R. Rinnan. 2010. Non-methane biogenic volatile organic compound emissions from a subarctic peatland under enhanced UV-B radiation. *Ecosystems* 13(6): 860–873.
- Fehsenfeld, F., J. Calvert, R. Fall, P. Goldan, A. B. Guenther, C. N. Hewitt, B. Lamb, et al. 1992. Emissions of volatile organic compounds from vegetation and the implications for atmospheric chemistry. *Global Biogeochemical Cycles* 6(4): 389–430.
- Geron, C., A. Guenther, T. Sharkey, and R. R. Arnsts. 2000. Temporal variability in basal isoprene emission factor. *Tree Physiology* 20(12): 799–805.
- Ghirardo, A., J. Xie, X. Zheng, Y. Wang, R. Grote, K. Block, J. Wildt, et al. 2016. Urban stress-induced biogenic VOC emissions and SOA-forming potentials in Beijing. *Atmospheric Chemistry and Physics* 16(5): 2901–2920.
- Guenther, A. B., P. R. Zimmerman, P. C. Harley, R. K. Monson, and R. Fall. 1993. Isoprene and monoterpene emission rate variability: Model evaluations and sensitivity analyses. *Journal of Geophysical Research: Atmospheres* 98(D7): 12609–12617.
- Hanson, D. T., S. Swanson, L. E. Graham, and T. D. Sharkey. 1999. Evolutionary significance of isoprene emission from mosses. *American Journal of Botany* 86(5): 634–639.
- Harley, P. C., R. K. Monson, and M. T. Lerdau. 1999. Ecological and evolutionary aspects of isoprene emission from plants. *Oecologia* 118(2): 109–123.
- Heck, M. A., V. M. Lüth, N. van Gessel, M. Krebs, M. Kohl, A. Prager, H. Joosten, et al. 2021. Axenic in vitro cultivation of 19 peat moss (*Sphagnum* L.) species as a resource for basic biology, biotechnology, and paludiculture. *New Phytologist* 229(2): 861–876.
- Holzinger, R., A. Kasper-Giebl, M. Staudinger, G. Schauer, and T. Röckmann. 2010. Analysis of the chemical composition of organic aerosol at the Mt. Sonnblick observatory using a novel high mass resolution thermal-desorption proton-transfer-reaction

- mass-spectrometer (hr-TD-PTR-MS). *Atmospheric Chemistry and Physics* 10: 10111–10128.
- Janson, R., C. De Serves, and R. Romero. 1999. Emission of isoprene and carbonyl compounds from a boreal forest and wetland in Sweden. *Agricultural and Forest Meteorology* 98–99(December): 671–681.
- Kollar, L. M., S. Kiel, A. J. James, C. T. Carnley, D. N. Scola, T. N. Clark, T. Khanal, et al. 2021. The genetic architecture of sexual dimorphism in the moss *Ceratodon purpureus*. *Proceedings of the Royal Society B: Biological Sciences* 288(1946): 20202908.
- Lantz, A. T., J. F. Cardillo, T. A. Gee, M. G. Richards, T. N. Rosenstiel, and A. J. Fisher. 2015. Biochemical characterization of an isoprene synthase from *Campylopus introflexus* (heath star moss). *Plant Physiology and Biochemistry* 94: 209–215.
- Lin, J., C. N. Kroll, D. J. Nowak, and E. J. Greenfield. 2019. A review of urban forest modeling: Implications for management and future research. *Urban Forestry & Urban Greening* 43(July): 126366.
- Materić, D., D. Bruhn, C. Turner, G. Morgan, N. Mason, and V. Gaudi. 2015. Methods in plant foliar volatile organic compounds research. *Applications in Plant Sciences* 3(12): 1500044.
- Monson, R. K., P. C. Harley, M. E. Litvak, M. Wildermuth, A. B. Guenther, P. R. Zimmerman, and R. Fall. 1994. Environmental and developmental controls over the seasonal pattern of isoprene emission from aspen leaves. *Oecologia* 99(3–4): 260–70.
- Monson, R. K., R. T. Jones, T. N. Rosenstiel, and J.-P. Schnitzler. 2013. Why only some plants emit isoprene. *Plant, Cell & Environment* 36(3): 503–516.
- Pankow, J. F., W. Luo, A. N. Melnychenko, K. C. Barsanti, L. M. Isabelle, C. Chen, A. B. Guenther, and T. N. Rosenstiel. 2012. Volatilizable biogenic organic compounds (VBOCs) with two dimensional gas chromatography-time of flight mass spectrometry (GC × GC-TOFMS): Sampling methods, VBOC complexity, and chromatographic retention data. *Atmospheric Measurement Techniques* 5: 345–361. <https://doi.org/10.5194/amt-5-345-2012>
- Prather, H. M., A. Casanova-Katny, A. F. Clements, M. W. Chmielewski, M. A. Balkan, E. E. Shortlidge, T. N. Rosenstiel, and S. M. Eppley. 2019. Species-specific effects of passive warming in an Antarctic moss system. *Royal Society Open Science* 6(11): 190744.
- Rinnan, R., L. L. Iversen, J. Tang, I. Vedel-Petersen, M. Schollert, and G. Schurgers. 2020. Separating direct and indirect effects of rising temperatures on biogenic volatile emissions in the Arctic. *Proceedings of the National Academy of Sciences, USA* 117 (51): 32476–32483.
- Romano, A., and G. B. Hanna. 2018. Identification and quantification of VOCs by proton transfer reaction time of flight mass spectrometry: An experimental workflow for the optimization of specificity, sensitivity, and accuracy. *Journal of Mass Spectrometry* 53: 287–295.
- Rosenstiel, T. N., E. E. Shortlidge, A. N. Melnychenko, J. F. Pankow, and S. M. Eppley. 2012. Sex-specific volatile compounds influence microarthropod-mediated fertilization of moss. *Nature* 489(7416): 431–433.
- Schallhart, S., P. Rantala, M. K. Kajos, J. Aalto, I. Mammarella, T. M. Ruuskanen, and M. Kulmala. 2018. Temporal variation of VOC fluxes measured with PTR-TOF above a boreal forest. *Atmospheric Chemistry and Physics* 18(2): 815–832.
- Sharkey, T. D., and F. Loreto. 1993. Water stress, temperature, and light effects on the capacity for isoprene emission and photosynthesis of kudzu leaves. *Oecologia* 95(3): 328–333.
- Sharkey, T. D., and R. K. Monson. 2017. Isoprene research: 60 years later, the biology is still enigmatic. *Plant, Cell & Environment* 40(9): 1671–1678.
- Shortlidge, E. E., S. B. Carey, A. C. Payton, S. F. McDaniel, T. N. Rosenstiel, and S. M. Eppley. 2021. Microarthropod contributions to fitness variation in the common moss *Ceratodon purpureus*. *Proceedings of the Royal Society B: Biological Sciences* 288: 20210119.
- Simon, H., J. Fallmann, T. Kropp, H. Tost, and M. Bruse. 2019. Urban trees and their impact on local ozone concentration: A microclimate modeling study. *Atmosphere* 10(3): 154.
- Spiegel, A., A. Kloskowski, W. Chrzanowski, and J. Namieśnik. 2013. Understanding solid-phase microextraction: Key factors influencing the extraction process and trends in improving the technique. *Chemical Reviews* 113(3): 1667–1685.
- Stein, S. E. 1999. An integrated method for spectrum extraction and compound identification from gas chromatography/mass spectrometry data. *Journal of the American Society for Mass Spectrometry* 10(8): 770–781.
- Tao, Y., and Y. M. Zhang. 2012. Effects of leaf hair points of a desert moss on water retention and dew formation: Implications for desiccation tolerance. *Journal of Plant Research* 125(3): 351–360.
- Vicheroová, E., R. Glinwood, T. Hájek, P. Šmilauer, and V. Ninkovic. 2020. Bryophytes can recognize their neighbours through volatile organic compounds. *Scientific Reports* 10(1): 7405.
- Yan, X., M.-X. He, Y. Guo, Y. Wang, J.-J. Han, and Q.-Z. Li. 2021. Study on volatile organic compounds of tree species and the influence on ozone and secondary organic aerosol. *IOP Conference Series: Earth and Environmental Science* 791(1): 012199.
- Yener, S., J. A. Sánchez-López, P. M. Granitto, L. Cappellin, T. D. Märk, R. Zimmermann, G. K. Bonn, et al. 2016. Rapid and direct volatile compound profiling of black and green teas (*Camellia sinensis*) from different countries with PTR-ToF-MS. *Talanta* 152(May): 45–53.

## SUPPORTING INFORMATION

Additional supporting information can be found online in the Supporting Information section at the end of this article.

**Appendix S1.** The five families and 50 species of moss gametophyte patches tested for isoprene emissions using GC-RGD.

**Appendix S2.** Data collected from *Atrichum undulatum* (AU), *Pogonatum urnigerum* (PU), and *Polytrichum juniperinum* (PJ) gametophytes for isoprene emissions using GC-RGD.

**Appendix S3.** Data collected from male and female *Polytrichum juniperinum* canopies using GC-RGD across 12 different field sites in Oregon with varying treatments of nitrogen.

**Appendix S4.** Data for isoprene collected from individual gametophytes of *Polytrichum juniperinum* using GC-RGD.

**Appendix S5.** Data for PTR-ToF-MS emission flux across four different moss species (*Antitrichia californica* [ANT], *Dicranoweisia cirrata* [DIC], *Polytrichum juniperinum* [POL], and *Racomitrium canescens* [RAC]) focusing on isoprene and monoterpenes.

**Appendix S6.** Chemical classes and compound identities for *Chorisodontium aciphyllum* collected using GC-ToF-MS.

**How to cite this article:** Brennan, D. L., L. M. Kollar, S. Kiel, T. Deakova, A. Laguerre, S. F. McDaniel, S. M. Eppley, E. T. Gall, and T. N. Rosenstiel. 2022. Measuring volatile emissions from moss gametophytes: A review of methodologies and new applications. *Applications in Plant Sciences* 10(2): e11468. <https://doi.org/10.1002/aps3.11468>